

Fast return-level estimates for flood insurance via an improved Bennett inequality for random variables with differing upper bounds

Anna Maria Barlow^{1*} and Chris Sherlock^{2†}

¹Institute for Stochastics and Applications, Universität Stuttgart, Germany.

²Department of Mathematics and Statistics, Lancaster University, UK.

Abstract

The k -year return levels of insurance losses due to flooding can be estimated by simulating and then summing a large number of independent losses for each of a large number of hypothetical years of flood events, and replicating this a large number of times. This leads to repeated realisations of the total losses over each year in a long sequence of years, from which return levels and their uncertainty can be estimated; the procedure, however, is highly computationally intensive. We develop and use a new, Bennett-like concentration inequality in a procedure that provides conservative but relatively accurate estimates of return levels at a fraction of the computational cost. Bennett's inequality provides concentration bounds on deviations of a sum of independent random variables from its expectation; it accounts for the different variances of each of the variables but uses only a single, uniform upper bound on their support. Motivated by the variability in the total insured value of insurance risks within a portfolio, we consider the case where the bounds on the support can vary by an order of magnitude or more, and obtain tractable concentration bounds. Simulation studies and application to a representative portfolio demonstrate the substantial improvement of our bounds over those obtained through Bennett's inequality. We then develop an importance sampling procedure that repeatedly samples the loss for each year from the distribution implied by the concentration inequality, leading to conservative estimates of the return levels and their uncertainty.

1 Introduction

The UK winter of 2015-16, which included Storms Desmond and Eva, saw more than 20,000 businesses and residential properties flood, resulting in insurance claims totalling

*anna-maria.barlow@mathematik.uni-stuttgart.de

†c.sherlock@lancaster.ac.uk

nearly £480 million. The floods of 2013-14 saw similar claims, and the floods in the summer of 2007 were even more costly. ¹

We are motivated by the problem of estimating the future insurance costs for a portfolio over the course of many hypothetical years, each of which may contain several flood events. The UK government’s 2015 solvency regulation (Swain and Swallow, 2015) requires specific information on the 200-year return level, the level of insurance payout over a year that is expected to be exceeded once in every 200-years on average; other return levels, from the 2-year to the 1000-year and above, are also of interest to insurers.

Each portfolio consists of a number of insurance *risks*, and each risk is partitioned into a number of *subrisks*. The procedure for estimating the distribution of each return level that is used by a funder of this work, for example, involves simulating flood events from a statistical extreme-value model (Lamb et al., 2010; Keef et al., 2013; Towe et al., 2019). Processing the output from the flood-event model results in, for each risk and each flood event, a probability, inherited by each subrisk within the risk, that the subrisk will suffer any flooding from the event and a distribution for the fraction of the total insured value that will be claimed conditional on the subrisk actually being flooded. Together these provide the *loss distribution*; see Taylor and Carter (2020) for the overarching simulation-based approach and Lamb et al. (2010) for a similar methodology applied to flood events. Importantly, the flood-event model is assumed to account for all of the dependence between losses at different subrisks; the individual losses are then assumed to be independent conditional on the individual loss distributions that arise from the model. Denoting the loss for the i th subrisk by Z_i , we are interested in the *total loss* for the portfolio over the year: $T_n = \sum_{i=1}^n Z_i$. Here $n = \sum_{j=1}^{n^{(ev)}} n_j$, where $n^{(ev)}$ is the number of flood events over the year and n_j is the number of subrisks with a non-zero probability of flooding during event j ². Centering the individual losses leads to $X_i = Z_i - \mathbb{E}[Z_i]$ ($i = 1, \dots, n$), and $T_n = \sum_{i=1}^n X_i + \sum_{i=1}^n \mathbb{E}[Z_i]$.

The portfolio can have 10^6 or more risks and n (the number of subrisks with a non-zero probability of flooding in a particular year of interest) can be very small or very large (see Barlow, 2021, for more details). Typically, $n_y = 1000$ or $n_y = 10000$ years worth of floods are simulated from the flood-event model and $M = 100$ or $M = 1000$ replicates of the loss for each year are simulated. This procedure is highly computationally intensive and can take 24 hours or more to complete for a given portfolio. This article presents a much faster, yet relatively accurate and provably conservative alternative methodology for estimating the k -year return levels for various k , based on an improvement to *Bennett’s* inequality.

Before introducing concentration inequalities, we first formalise the set up that will be used throughout this article. Let X_1, \dots, X_n be independent random variables with

$$\mathbb{E}X_i = 0 \quad \text{and} \quad \text{Var}[X_i] = \sigma_i^2, \tag{1}$$

and define

$$S_n = \sum_{i=1}^n X_i \quad \text{and} \quad \overline{\sigma^2} = \frac{1}{n} \sum_{i=1}^n \sigma_i^2. \tag{2}$$

¹<https://www.gov.uk/government/publications/floods-of-winter-2015-to-2016-estimating-the-costs>

²For simplicity here we ignore the possibility that a subrisk subject to two floods in a year might have an altered loss distribution for the second flood, though it is possible to deal with this.

Losses due to flooding typically possess the following two properties:

1. The total value insured for a given risk, and hence the maximum loss from that risk, varies from risk to risk, often by more than an order of magnitude.
2. In a given event, for most, but not all, risks the probability of flooding is small, and even conditional on flooding, the total damage is often much less than the value insured; hence the variance for that risk is smaller than might be guessed given the value insured.

The first property suggests that Hoeffding’s inequality might be appropriate, since it accounts for the individual variations in support:

Theorem 1. (Hoeffding, 1963, Theorem 2) *Let X_1, \dots, X_n and S_n be as defined in and above (1) and (2) and let $\mathbb{P}(a_i \leq X_i \leq c_i) = 1$ for some a_1, \dots, a_n and c_1, \dots, c_n . Then*

$$\frac{1}{n} \log \mathbb{P}(S_n \geq nt) \leq -\frac{2t^2}{\frac{1}{n} \sum_{i=1}^n (c_i - a_i)^2}.$$

The second property suggests the use of Bennett’s inequality, which, unlike Hoeffding’s inequality takes the variances into account and, indeed, allows for different variances for each risk, but does not account for the variations in support, assuming that for some $c_* > 0$,

$$\mathbb{P}(X_i \leq c_*) = 1 \tag{3}$$

for each i in $1, \dots, n$

Theorem 2. (Bennett, 1962) *Let X_1, \dots, X_n be independent random variables subject to (1) and (3). Then for any $t > 0$,*

$$\frac{1}{n} \log \mathbb{P}(S_n > nt) \leq -\frac{\overline{\sigma^2}}{c_*^2} h\left(\frac{c_* t}{\overline{\sigma^2}}\right), \tag{4}$$

where $h(u) = (1 + u) \log(1 + u) - u$ and S_n and $\overline{\sigma^2}$ are as defined in (2).

Since its inception, Bennett’s inequality has been tightened slightly (Hoeffding (1963), Theorem 3; Zheng (2018)) subject to the same conditions as the original theorem, and tightened further subject to additional moment information on the individual X_i (e.g. Pinelis and Utev, 1990; Light, 2021; Bentkus and Juškevičius, 2008; Pinelis, 2014). All of the listed articles, however, require a uniform upper bound (3); for an exception, see Bennett (1962) Equation 2c, mentioned in Section 5 of this article.

Neither inequality is entirely satisfactory as each fails to account for an important property of the components of the sum that makes up the total loss in a year. We focus on Bennett’s inequality and tighten it by accounting for the different supports of the individual subrisks.

Given a bound on the probability of the loss for a particular year exceeding a given amount, our first methodological contribution is to avoid simulating the individual losses at each individual subrisk for each event for that year and summing them; instead, we simulate from

the distribution implied by the bound on the sum for that year. Repeating for each year leads to conservative estimates and upper prediction limits for the k -year return levels for all required k . This procedure can be repeated using equivalent concentration bounds on the lower tails of the yearly losses. Whilst typically faster than direct Monte Carlo simulation, the method does not give the desired improvement in computational effort. Our second methodological contribution is an importance-sampling resampling scheme that speeds up the procedure by several orders of magnitude compared with the standard methodology.

Section 2 of this article describes the new Bennett-like inequalities which allow for different supports for the individual components of the sum. In Section 3 the new bounds are compared with existing bounds and estimates in various binary-data scenarios and in four indicative years from a realistic, simulated portfolio and set of flood events. The new scheme, including the importance-sampling resampling method is described in Section 4, and timings and estimates of the k -year return levels are compared with those from the standard scheme using the full portfolio. The article concludes with a discussion.

2 Bennett inequalities allowing for different support

Suppose that we have information on the support of each variable, replacing (3) with

$$\mathbb{P}(X_i \leq c_i) = 1, \quad i = 1, \dots, n. \quad (5)$$

Let Z_i be the loss from an individual risk during a large event, such as a flood. Then $0 \leq Z_i \leq b_i$, where b_i is the maximum value insured. Defining $X_i = Z_i - \mathbb{E}Z_i$ we see that (5) holds with $c_i = b_i - \mathbb{E}[Z_i]$. Clearly, (4) continues to hold in this case, with $c_* = \max_{i=1, \dots, n} c_i$; however, as discussed in Section 1, and shown in the numerical experiments of Section 3, Bennett's inequality using c_* is unsatisfactory.

Fundamental to the proofs of Theorems 1 and 2 and to many of the improvements upon them is the Chernhoff bound (e.g. Boucheron et al., 2013): for any $\lambda > 0$,

$$\mathbb{P}(S_n \geq nt) = \mathbb{P}(\exp(\lambda S_n) \geq \exp(\lambda nt)) \leq \exp(-\lambda nt) \mathbb{E}[\exp(\lambda S_n)],$$

by Markov's inequality. Thus

$$\frac{1}{n} \log \mathbb{P}(S_n \geq nt) \leq \inf_{\lambda > 0} \left\{ \frac{1}{n} \log \mathbb{E}[\exp(\lambda S_n)] - \lambda t \right\}. \quad (6)$$

Theorem 2 uses the following bound on the moment generating function of S_n in (6):

$$\frac{1}{n} \log \mathbb{E}[\exp(\lambda S_n)] \leq \lambda^2 \overline{\sigma^2} f_2(\lambda c_*),$$

where, for $k = 1, 2, \dots$,

$$f_k(u) = \frac{1}{u^k} \left\{ \exp(u) - \sum_{j=0}^{k-1} \frac{u^j}{j!} \right\} = \sum_{j=0}^{\infty} \frac{u^j}{(j+k)!}. \quad (7)$$

Our result relies on the following improved bound, proved in Section 2.1:

$$\begin{aligned} \frac{1}{n} \log \mathbb{E} [\exp(\lambda S_n)] &\leq \frac{1}{2} \lambda^2 \overline{\sigma^2} + \lambda^2 K \left\{ f_2(\lambda c_*) - \frac{1}{2} \right\} - \lambda^4 c_*^2 K_1 f_4(\lambda c_*) \\ &=: B(\lambda; c_*, \overline{\sigma^2}, K, K_1), \end{aligned} \quad (8)$$

where,

$$K = \frac{1}{n} \sum_{i=1}^n \sigma_i^2 \frac{c_i}{c_*} \quad \text{and} \quad K_1 = \frac{1}{n} \sum_{i=1}^n \sigma_i^2 \frac{c_i}{c_*} \left(1 - \frac{c_i}{c_*} \right). \quad (9)$$

Bound (8) relies only on the summary statistics c_* , $\overline{\sigma^2}$, K and K_1 , and the resulting minimisation problem can be efficiently solved numerically. Alternatively, the looser bound obtained by omitting the term in K_1 leads to a tractable minimisation problem with a solution in terms of Lambert's W function (e.g. Corless et al., 1996), which we denote by \mathcal{W} ; the solution can then be substituted into (8) or into the looser bound. These considerations lead to our main result:

Theorem 3. *Let X_1, \dots, X_n be independent random variables subject to (1) and (5). Define S_n , $\overline{\sigma^2}$, B , K and K_1 as in (2), (8) and (9), and let $c_* = \max_{i=1, \dots, n} c_i$. For any $t > 0$,*

$$\frac{1}{n} \log \mathbb{P}(S_n \geq nt) \leq B_1(t) := \inf_{\lambda > 0} \{ B(\lambda; c_*, \overline{\sigma^2}, K, K_1) - \lambda t \} \quad (10)$$

$$\leq B_2(t) := B(\lambda_*; c_*, \overline{\sigma^2}, K, K_1) - \lambda_* t \quad (11)$$

$$\leq B_3(t) := B(\lambda_*; c_*, \overline{\sigma^2}, K, 0) - \lambda_* t \quad (12)$$

$$= \inf_{\lambda > 0} \{ B(\lambda; c_*, \overline{\sigma^2}, K, 0) - \lambda t \}, \quad (13)$$

where

$$\lambda_* = \frac{1}{c_*} \left[\frac{K + tc_*}{\overline{\sigma^2} - K} - \mathcal{W} \left(\frac{K}{\overline{\sigma^2} - K} \exp \left(\frac{K + tc_*}{\overline{\sigma^2} - K} \right) \right) \right]. \quad (14)$$

2.1 Proofs and a lower bound on the possible improvement

This section proves Theorem 3. We first note some properties of the function f_2 ; from the first of these we prove (8) and bound the discrepancy from a tightest-possible Bennett-like bound, giving a lower bound on the best possible Bennett-like concentration inequality that accounts for the individual c_i . From (8) and Proposition 1(ii) we derive our new concentration inequalities.

Proposition 1. *(i) The Maclaurin series for $f_2(u)$ is $\sum_{j=0}^{\infty} u^j / (j+2)!$, and (ii) $f_2'(u) = (1 - 2/u)f_2(u) + 1/u$.*

Lemma 1. *The bound (8) holds. Furthermore, a lower bound on the upper bound on $\frac{1}{n} \log \mathbb{E} [\exp(\lambda S_n)]$ that could be achieved if the methodology which generates Theorem 2 could take (5) into account exactly, is*

$$B_{\text{lb}} := B(\lambda; c_*, \overline{\sigma^2}, K, K_1) - \lambda^5 c_*^3 (K - K_1) f_5(\lambda c_*). \quad (15)$$

Proof. As in the proof of Bennett's inequality, for any random variable X with $\mathbb{E}[X] = 0$ and $\mathbb{P}(X \leq c) = 1$,

$$\begin{aligned}\mathbb{E}[\exp(\lambda X)] &= \mathbb{E}\left[\sum_{j=0}^{\infty} \frac{\lambda^j}{j!} X^j\right] = \sum_{j=0}^{\infty} \frac{\lambda^j}{j!} \mathbb{E}[X^j] = 1 + \sum_{j=2}^{\infty} \frac{\lambda^j}{j!} \mathbb{E}[X^j] \\ &\leq 1 + \sum_{j=2}^{\infty} \frac{\lambda^j}{j!} \mathbb{E}[X^2] c^{j-2} = 1 + \lambda^2 \text{Var}[X] f_2(\lambda c) \\ &\leq \exp\{\lambda^2 \text{Var}[X] f_2(\lambda c)\}.\end{aligned}$$

Again, as in the proof of Bennett's inequality, since the X_i are independent,

$$\frac{1}{n} \log \mathbb{E}[\exp(\lambda S_n)] = \frac{1}{n} \sum_{i=1}^n \log \mathbb{E}[\exp(\lambda X_i)] \leq \lambda^2 \frac{1}{n} \sum_{i=1}^n \sigma_i^2 f_2(\lambda c_i). \quad (16)$$

Now, let

$$h(u) = \frac{1}{2!} + \frac{u}{3!} = f_2(u) - \sum_{j=2}^{\infty} \frac{u^j}{(j+2)!},$$

by Proposition 1. Rearranging the above also shows that the infinite sum is absolutely convergent for all finite u . Since h is linear, $h(u) = (1 - u/u_*)h(0) + (u/u_*)h(u_*)$. Rearranging, and then considering only $0 \leq u \leq u_*$, we obtain:

$$\begin{aligned}f_2(u) &= \left(1 - \frac{u}{u_*}\right) f_2(0) + \frac{u}{u_*} f_2(u_*) + \sum_{j=2}^{\infty} \frac{u^j}{(j+2)!} - \frac{u}{u_*} \sum_{j=2}^{\infty} \frac{u_*^j}{(j+2)!} \\ &= \left(1 - \frac{u}{u_*}\right) f_2(0) + \frac{u}{u_*} f_2(u_*) + u^2 \sum_{j=0}^{\infty} \frac{u^j}{(j+4)!} - uu_* \sum_{j=0}^{\infty} \frac{u_*^j}{(j+4)!} \quad (17)\end{aligned}$$

$$\begin{aligned}&\leq \left(1 - \frac{u}{u_*}\right) f_2(0) + \frac{u}{u_*} f_2(u_*) + u^2 \sum_{j=0}^{\infty} \frac{u_*^j}{(j+4)!} - uu_* \sum_{j=0}^{\infty} \frac{u_*^j}{(j+4)!} \\ &= f_2(0) + \frac{u}{u_*} \{f_2(u_*) - f_2(0)\} - \frac{u}{u_*} \left\{1 - \frac{u}{u_*}\right\} u_*^2 f_4(u_*), \quad (18)\end{aligned}$$

where the inequality follows because $0 \leq u \leq u_*$. Thus

$$\begin{aligned}\frac{1}{n} \lambda^2 \sum_{i=1}^n \sigma_i^2 f_2(\lambda c_i) &\leq \lambda^2 \frac{1}{n} \sum_{i=1}^n \left\{ \sigma_i^2 f_2(0) + \sigma_i^2 \frac{c_i}{c_*} \{f_2(\lambda c_*) - f_2(0)\} - \sigma_i^2 \frac{c_i}{c_*} \left(1 - \frac{c_i}{c_*}\right) \lambda^2 c_*^2 f_4(\lambda c_*) \right\} \\ &= \lambda^2 \bar{\sigma}^2 f_2(0) + \lambda^2 K \{f_2(\lambda c_*) - f_2(0)\} - \lambda^4 c_*^2 K_1 f_4(\lambda c_*),\end{aligned}$$

which simplifies to (8) as $f_2(0) = 1/2$.

Next, the discrepancy between the bound we use, (18), and $f_2(u)$ in (17) is

$$u^2 \sum_{j=0}^{\infty} \frac{u_*^j}{(j+4)!} \left\{1 - \frac{u^j}{u_*^j}\right\} = u^2 \sum_{j=1}^{\infty} \frac{u_*^j}{(j+4)!} \left\{1 - \frac{u^j}{u_*^j}\right\} \leq u^2 u_* \sum_{j=0}^{\infty} \frac{u_*^j}{(j+5)!} = \frac{u^2}{u_*^2} u_*^3 f_5(u_*).$$

Hence

$$B(\lambda; c_*, \overline{\sigma^2}, K, K_1) - \frac{1}{n} \lambda^2 \sum_{i=1}^n \sigma_i^2 f_2(\lambda c_i) \leq \frac{1}{n} \lambda^2 \sum_{i=1}^n \sigma_i^2 \frac{c_i^2}{c_*^2} (\lambda c_*)^3 f_5(\lambda c_*) = \lambda^5 c_*^3 (K - K_1) f_5(\lambda c_*).$$

□

2.1.1 Proof of Theorem 3

Remark 1. Since $0 \leq c_i \leq c_*$, we have $K_1 \leq K \leq \overline{\sigma^2}$.

We now prove Theorem 3.

Proof. The tightest bound, (10), follows directly from (6) and (8). Since $K_1 > 0$, setting $K_1 = 0$ gives the looser bound (13), which we solve to obtain λ_* , leading directly to (11) and (12). Taking (8) with $K_1 = 0$ and using Proposition 1 (ii),

$$\begin{aligned} B'(\lambda; c_*, \overline{\sigma^2}, K, 0) &= \lambda \overline{\sigma^2} + 2\lambda K \left\{ f_2(\lambda c_*) - \frac{1}{2} \right\} + \lambda^2 K c_* f'(\lambda c_*) \\ &= \lambda \overline{\sigma^2} + 2\lambda K \left\{ f_2(\lambda c_*) - \frac{1}{2} \right\} + \lambda^2 K c_* \left\{ \left(1 - \frac{2}{\lambda c_*}\right) f_2(\lambda c_*) + \frac{1}{\lambda c_*} \right\} \\ &= \lambda \overline{\sigma^2} + \lambda^2 K c_* f_2(\lambda c_*) = \lambda \overline{\sigma^2} + \frac{K}{c_*} \{ \exp(\lambda c_*) - 1 - \lambda c_* \} \\ &= \lambda \left(\overline{\sigma^2} - K \right) - \frac{K}{c_*} + \frac{K}{c_*} \exp(\lambda c_*) \end{aligned}$$

Thus, to minimise $B(\lambda) - \lambda t$ we must solve

$$\frac{K}{c_*} \exp(\lambda c_*) = -\lambda \left(\overline{\sigma^2} - K \right) + \left(t + \frac{K}{c_*} \right).$$

Since the left hand side is increasing, with an intercept at $\lambda = 0$ which is strictly less than the intercept of the right hand side, and the right hand side is decreasing (see Remark 1), there is exactly one solution on $[0, \infty)$. We must solve

$$\begin{aligned} K \exp(\lambda c_*) &= (K + t c_*) - \lambda c_* (\overline{\sigma^2} - K) \iff \frac{K}{\overline{\sigma^2} - K} = \left[\frac{K + t c_*}{\overline{\sigma^2} - K} - \lambda c_* \right] \exp(-\lambda c_*) \\ &\iff \frac{K}{\overline{\sigma^2} - K} \exp\left(\frac{K + t c_*}{\overline{\sigma^2} - K}\right) = \left[\frac{K + t c_*}{\overline{\sigma^2} - K} - \lambda c_* \right] \exp\left(\frac{K + t c_*}{\overline{\sigma^2} - K} - \lambda c_*\right). \end{aligned}$$

Thus

$$\frac{K + t c_*}{\overline{\sigma^2} - K} - \lambda c_* = \mathcal{W}\left(\frac{K}{\overline{\sigma^2} - K} \exp\left(\frac{K + t c_*}{\overline{\sigma^2} - K}\right)\right),$$

which leads to (14). □

3 Numerical experiments

3.1 Toy examples

We construct four toy scenarios for comparing our bounds by, in each case, simulating $n = 10^5$ random distributions as follows. For $i = 1, \dots, n$, simulate b_i from some non-negative distribution, G , and simulate $p_i \sim \text{Beta}(\alpha, \beta)$ for some $\alpha > 0$ and $\beta > 0$. We imagine $Z_i = b_i * \text{Bern}(p_i)$, where Bern represents the Bernoulli distribution. From Z_i we create the centred random variable $X_i = Z_i - b_i p_i$, and we are interested in $S_n = \sum_{i=1}^n X_i$. The individual upper bounds are $c_i = b_i(1 - p_i)$ and the variances are $\sigma_i^2 = b_i^2 p_i(1 - p_i)$.

Our motivation arises from cases where most of the random variables are likely to take low values, so for the first three experiments we take $\alpha = 1$ and $\beta = 10$. Scenarios of interest to us also have fewer larger c_i than there are smaller c_i and we consider three tail scenarios: (i) light tails, where $B_i = |Z_i|$, with $Z_i \sim \text{N}(0, 1)$; (ii) exponential tails, where $B_i \sim \text{Exp}(1)$ and (iii) heavy tails, where $B_i \sim \text{Pareto}$ with a shape parameter of 4. Our final scenario (iv) uses the intermediate tail behaviour ($B_i \sim \text{Exp}(1)$) and has $P_i \sim \text{Unif}(0, 1)$ ($\alpha = \beta = 1$). We vary t from 0 to such a value that our tightest bound gives $\frac{1}{n} \log \mathbb{P}(S_n > nt) \approx -0.025$; even with n as low as 600, this covers events down to a probability of less than 10^{-6} .

Theorem 3 does not require that the random variables X_i be bounded below; however, when they are bounded below by $a_i \leq 0$, Hoeffding’s inequality (Theorem 1) provides an alternative bound which takes account of the individual ranges, but not the individual variances. In our experiments, we also evaluate the Hoeffding bound for comparison, as well as the tightening of Bennett’s bound in Theorem 3 of Hoeffding (1963), which is the tightest possible under the conditions of Theorem 2. The latter is not shown in the plots as in all scenarios it was visually indistinguishable from Bennett’s bound.

Figure 1 shows the bounds plotted against t , and includes the corresponding large- n approximation from the central limit theorem, $\frac{1}{n} \log \mathbb{P}(S_n \geq nt) \sim -0.5t^2/\sigma^2$, which, for large n , may be considered an upper bound on what might be achievable by any concentration inequality. We also include bounds derived from B_{lb} , which bounds the potential improvement from using an idealised Bennett-like inequality that would cost $\mathcal{O}(n)$ to evaluate for each λ . All of the new bounds improve on the Bennett bound, accounting for a substantial fraction of the gap between the Bennett bound and the approximation from the central limit theorem. Furthermore, the possibility for further improvement by approaching a “perfect” Bennett-like bound is small. All of the new bounds are also substantially tighter than the Hoeffding bound over the range of t values considered. Using the λ_* obtained from minimising (12) within the tighter bound (11) appears to offer a non-negligible improvement over (12).

3.2 Our portfolios

Our simulated ‘standard portfolio’ is itself based upon a smaller portfolio provided by JBA Risk Management, which consisted of 10,000 risks and 181,789 subrisks. For anonymisation purposes, this was transformed and then perturbed to become our ‘small portfolio’.

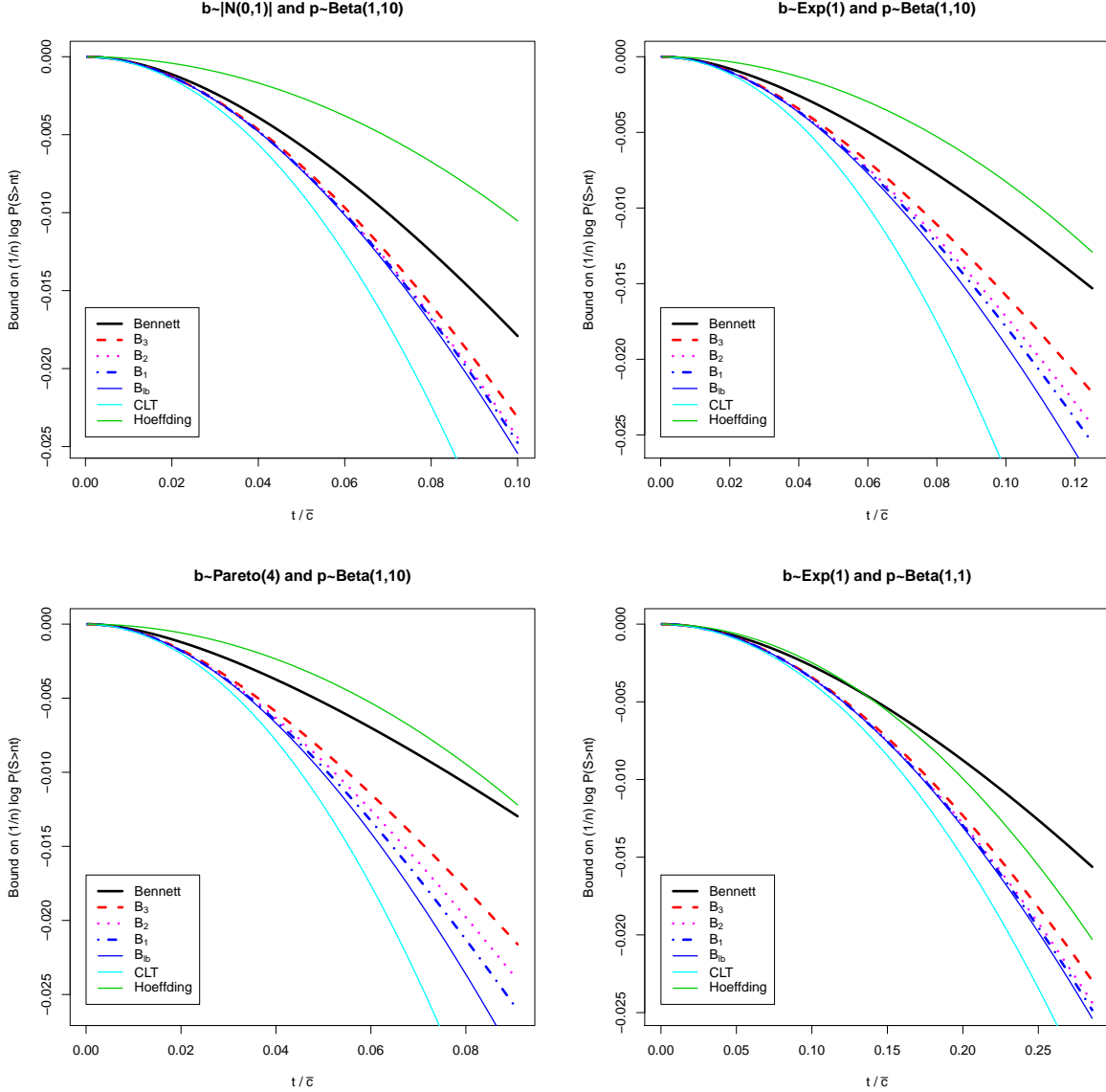


Figure 1: Comparison of bounds on $\frac{1}{n} \log \mathbb{P}(S_n \geq nt)$ plotted against t/\bar{c} : Bennett (black solid); B_1 (10) in blue dot-dash; B_2 (11) in magenta dotted and B_3 (12) in red dashed. Other solid lines are: the large- n approximation from the central limit theorem (cyan), the Hoeffding bound (green) and a lower bound, B_{lb} , on the best possible “Bennett”-like bound, obtained from (15) (solid blue). The four panels correspond to the scenarios as follows: (i) top left, (ii) top right, (iii) bottom left, and (iv) bottom right.

Table 1: Statistics for the years with the lower quartile (A), median (B), upper quartile (C) and maximum (D) expected loss: number of events in that year, $n^{(ev)}$, expected loss ($\mathbb{E}[S_n]$), number of (subrisk,event) combinations in that year with a non-zero probability of flooding ($n^{(p>0)}$), mean probability of flooding amongst this (subrisks,event) set (\bar{p}), and mean over this set of the expected fraction of the insured value that would be lost were the subrisk to flood ($\bar{\mu}$). Subrisks with a non-zero probability of flooding more than once during the year are treated as separate subrisks for the purposes of these statistics.

Year	$n^{(ev)}$	$\mathbb{E}[S_n]$ (£k)	$n^{(p>0)}$	\bar{p}	$\bar{\mu}$ (%)
A	7	739	3 220	0.041	9.92
B	12	3 923	2 480	0.127	7.86
C	10	13 740	8 690	0.168	9.06
D	11	266 800	64 860	0.199	10.72

Furthermore, 1000 (hypothetical) years of output from the flood-event model supplied, for each flood event and each risk, the probability of flooding and the (beta) distribution of the fraction of the total-insured value that would be claimed were flooding to occur. Recall that each risk is partitioned into subrisks, with the total insured value split evenly across the subrisks and with the loss from each subrisk treated independently of the losses from all other subrisks.

The portfolio provided by JBA was much smaller than typical portfolios so from it we bootstrapped a portfolio with exactly ten times the total numbers of risks and subrisks; we refer to this as the standard portfolio. If in the original portfolio, subrisk S was part of risk R then the simulation ensured that in the standard portfolio each copy of subrisk S would be part of a copy of risk R. In the standard portfolio, the lowest insured value for a subrisk was £15,559.14 and the highest was £379,382.60. In an analogous manner, we also created a ‘large portfolio’ which has ten times the number of risks as our standard portfolio.

Table 1 provides summary statistics for four particular years from our standard portfolio: the years with the first, second and third quartiles and maximum of the expected loss, respectively labelled A, B, C and D. Across these four years, the mean number of non-zero terms summed varies from 132 (year A) to 12907 (year D).

3.3 Flood example

For each of the years A, B, C and D, Figure 2 plots the Bennett and Hoeffding bounds and our bounds B_1 (10), B_2 (11) and B_3 (12), as well as the estimate from the central limit theorem and a 90% confidence interval based on 20,000 simulations from the true distribution. As expected, the Hoeffding inequality performs very poorly, and our bounds offer a substantial improvement on the Bennett bound. Bound B_2 is almost indistinguishable from B_1 ; for Years C and D, B_1 and B_2 are close to the best achievable by extensions of our method, and even for years A and B, the possible room for further improvement is half or less of that already achieved over the Bennett bound. Since we are especially interested in high return levels, it is the range of years from the upper quartile to the maximum (of

expected loss) that is most important. The approximation due to the central limit is so poor, even though $n > 200$ in all cases, because the individual loss distributions are so highly skewed, with a high probability of no loss.

An upper bound on $\frac{1}{n} \log \mathbb{P}(S \leq nt)$ is obtained by applying our bounds to $-S$. Figure 5 in Appendix B is the equivalent of Figure 2 but for the bounds on the lower tail probabilities. In all cases our bound is much closer to the Monte Carlo and the central limit-theorem estimates than for the upper tail, and is only slightly closer than the Bennett bound. As with the plots for the upper tail, the Bennett bound is much tighter than the Hoeffding bound. In contrast to X_i which are typically strongly right skewed meaning that occasional large values are important, $-X_i$ is typically heavily skewed to the left, and so the upper tail of the sum has a behaviour much closer to that predicted by the central limit theorem.

4 Estimation of return levels

We now describe the use of concentration inequalities to bound the y -year return level. We first describe the standard procedure used by our funder and by the wider insurance/consultation industry (e.g. Taylor and Carter, 2020; Lamb et al., 2010), and then our new methodology.

Both methods start from n_y years of simulated storm events, where, typically $n_y = 1000$ or $n_y = 10000$. Each year, y , contains $n_y^{(ev)}$ events, and each event, (y, e) , has $n_{y,e}^{(p>0)}$ risks with a non-zero probability of flooding. For each combination of year and event number for that year, each risk that might flood is associated with with a probability $p_{y,e,r}$ of flooding, and a beta distribution with specified parameters unique to this (y, e, r) combination, corresponding to a distribution on the claim as a fraction of the insured value. Let $Z_{y,e,r}^{(j)}$ correspond to the j th realisation from a sequence of independent random variables each of which is 0 with a probability of $1 - p_{y,e,r}$ and is otherwise drawn from the beta variable unique to that (y, e, r) combination.

Each risk, r has a total insured value b_r , which is divided evenly between its $n_r^{(sub)}$ subrisks. Each subrisk, s , inherits $p_{y,e,r}$ and the beta distribution from their parent risk $r(s)$.

For $y \in \{1, \dots, n_y\}$, the loss for year y is

$$T_y = \sum_{e=1}^{n_y^{(ev)}} \sum_{r=1}^{n_{y,e}^{(p>0)}} \frac{b_r}{n_r^{(sub)}} \sum_{s=1}^{n_r^{(sub)}} Z_{y,e,r}^{(s)}. \quad (19)$$

Consider the order statistics: $T_{(1)}, \dots, T_{(n_y)}$. The k -year return level is the value that will be exceeded on average every k years, and our best estimate of its distribution is the distribution of $T_{(n_y/k)}$. Typically, interest lies in $k = 2, 5, 10, 20, 50, 100, 200$ and 500 .

Henceforth, we set $\mu_{y,e,r} = p_{y,e,r} \alpha_{y,e,r} / (\alpha_{y,e,r} + \beta_{y,e,r})$ and $X_{y,e,r}^{(s)} = b_r \{Z_{y,e,r}^{(s)} - \mu_{y,e,r}\} / n_r^{(sub)} \leq b_r \{1 - \mu_{y,e,r}\} / n_r^{(sub)}$, and consider the equivalent sum S_y of the $X_{y,e,r}^{(s)}$.

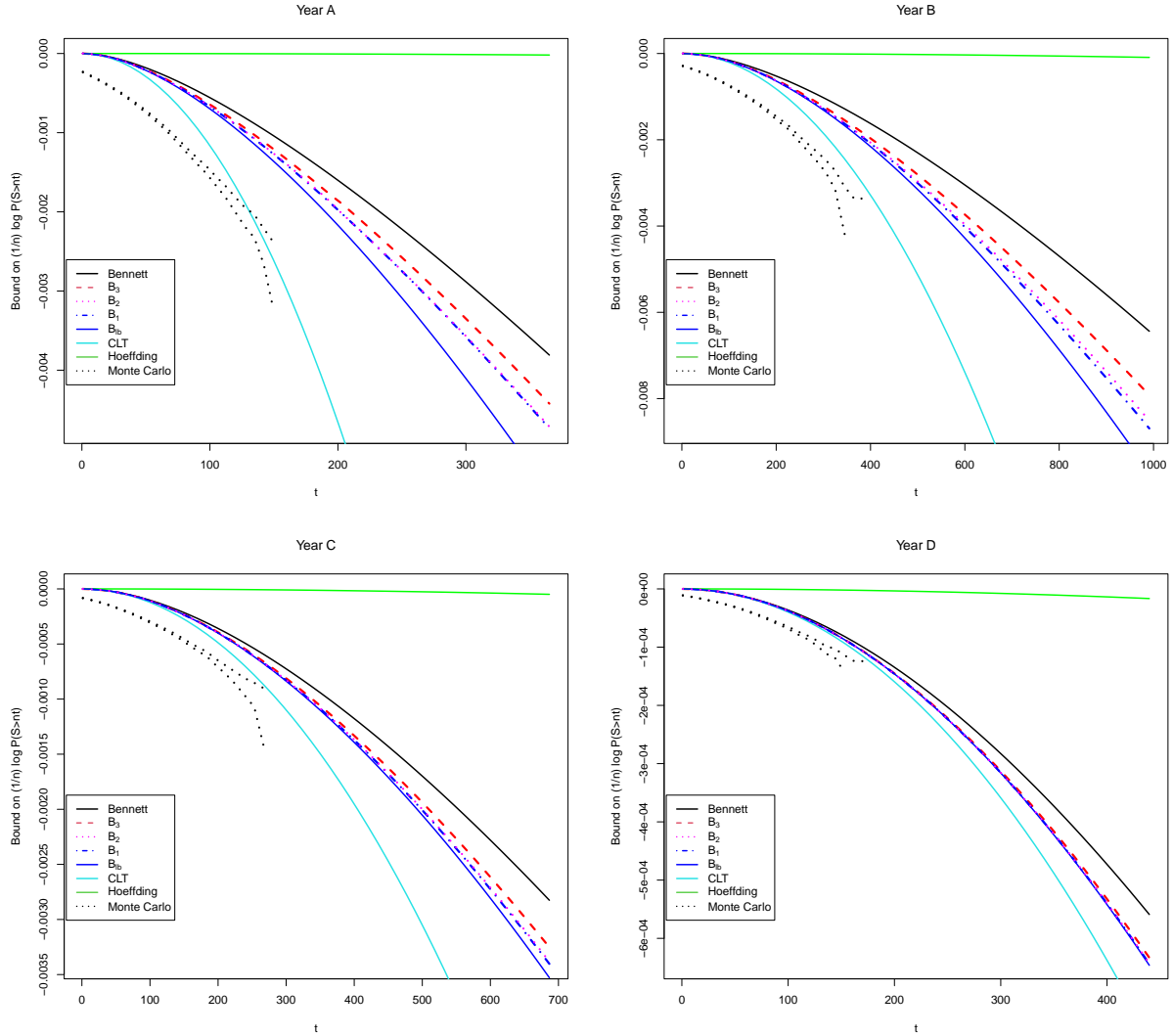


Figure 2: Comparison of bounds on $\frac{1}{n} \log \mathbb{P}(S_n - \mathbb{E}[S_n] \geq nt)$ plotted against t : Bennett (black solid); B_1 (10) in blue dot-dash; B_2 (11) in magenta dots and Equation (12), denoted B_3 , in red dashed. Other solid lines are: the large- n approximation from the central limit theorem (cyan) and the Hoeffding bound (green). The dotted lines show 90% CIs based on 20000 Monte Carlo simulations from the true distribution. The four panels correspond respectively to Years A, B, C and D.

4.1 The standard method

The standard method repeatedly simulates the loss at every single risk for every single flood event. For each combination of (y, e, r, s) a realisation $x_{y,e,r}^{(s)}$ of the random variable $X_{y,e,r}$ is simulated independently of all other realisations, leading, via (19), to realisations s_y ($y = 1, \dots, n_y$). The corresponding realisation of return level k is $q_k = s_{(n_y/k)}$, and this can be obtained for each k of interest from the simulated s_y values.

Let M be the number of replicates required; typically $M = 100$ or 1000 . Repeating the above procedure M times gives a sample of size M from the distribution of each return level of interest, from which point estimates (usually the mean) and an approximate 95% (quantile-based) interval can be obtained.

Each return level is a deterministic function of the parameters in the flood-level model and the model that converts flood levels to loss distributions. These parameters are fixed at their estimated values for each repeat simulation of all n_y years, so the Monte Carlo interval does not take parameter uncertainty into account. Indeed, if the model with the estimated parameters were the true loss generating process then, in the limit as $M \rightarrow \infty$, the estimated interval for the k -year return level is such that the probability that the true (n_y/k) th highest level in n_y years is in the interval is 0.95. Thus, the interval can be thought of as a prediction interval for r_k provided that the model and parameters that are used are the truth. The fact that it only allows for simulation uncertainty and not parameter or model uncertainty will resurface in the discussion (see Section 5.2).

The standard method is exceedingly costly, computationally, as in real scenarios, where the portfolio size might be between 10^5 and 5×10^6 , it involves the simulation of multiple replicates of an exceedingly large number of random variables (even accounting for the fact that we can automatically set $X_{y,e,r} = 0$ for risks with no chance of flooding during a particular event). If $n^{(ev)}$, $n^{(p>0)}$ and $n^{(sub)}$ are, respectively, the mean number of events per year, risks with non-zero probability of flooding per event and subrisks per risk, and \bar{p} is the average probability of flooding amongst subrisks where this is non-zero, then the number of simulations is $\mathcal{O}(M n_y n^{(ev)} n^{(p>0)} \bar{p} n^{(sub)})$.

4.2 A new approach

Some aspects of the new approach mimic the standard approach: M replicates for the total losses on each of the n_y years are obtained. However, these replicates do not require individual simulations of every single loss at every single subrisk.

Instead of a sample from the distribution of S_y with (unknown and intractable) cumulative distribution function (cdf) F_y , we sample from the distribution of random variables S_y^- and S_y^+ with known cdfs F_y^- and F_y^+ , which are ordered as follows:

$$F_y^+(s) \leq F_y(s) \leq F_y^-(s). \quad (20)$$

Since both F_y^- and F_y^+ are known, we may simulate from these simultaneously via the inverse cdf method: simulate a realisation u from a $\text{Uniform}(0, 1)$ random variable and then set s_y^- and s_y^+ to be the solutions to $F_y^-(s_y^-) = u$ and $F_y^+(s_y^+) = u$. As shown in Figure 3,

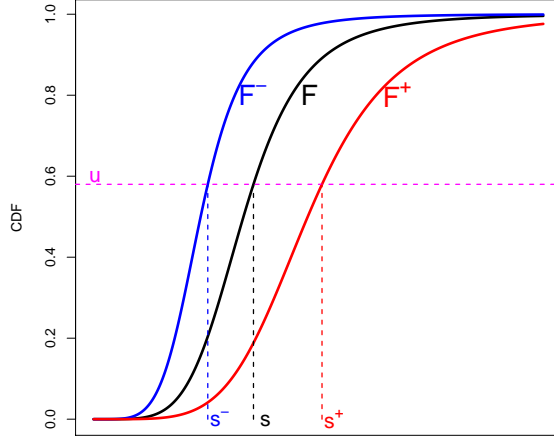


Figure 3: Illustration of a cumulative distribution function (cdf) F , the upper and lower bounds F^- and F^+ which are also cdfs, and the three resulting realisations, s , s^- and s^+ , for a particular value of u .

this implies that $s_- \leq s \leq s_+$, where $s = F^{-1}(u)$ is the hypothetical simulated value from the true distribution of S_y that would be obtainable if its cdf were known.

The distribution functions F^- and F^+ arise directly from concentration inequalities as follows. Suppose that we have two concentration inequalities: $\mathbb{P}(S \leq s) \leq g_{lo}(s)$ and $\mathbb{P}(S \geq s) \leq g_{hi}(s)$. Then

$$F^-(s) = g_{lo}(s) \geq \mathbb{P}(S \leq s) = F(s) \quad (21)$$

$$F^+(s) = 1 - g_{hi}(s) \leq 1 - \mathbb{P}(S \geq s) = F(s). \quad (22)$$

The following is repeated M times: for each y , a realisation, u_y , from a **Uniform**(0,1) distribution is sampled, and from this concurrent realisations from s_y^- and s_y^+ are obtained via the inverse-cdf method. The corresponding realisations of the k -year return level are obtained from the order statistics: $q_k^- = s_{(n_y/k)}^-$ and $q_k^+ = s_{(n_y/k)}^+$.

Since $s_y^- \leq s_y \leq s_y^+$ for each y , we have $q_k^- \leq q_k \leq q_k^+$, where q_k is the return level that would have been obtained if we had sampled from the true distribution of S_1, \dots, S_{n_y} via the inverse-cdf method.

The point estimate that would have been obtained can be bracketed between the mean (over the M replicates) of the q_k^- and the mean of the q_k^+ . A conservative 95% prediction interval can be obtained from the estimated 2.5% quantile of the q_k^- and the 97.5% quantile of the q_k^+ .

Typically $g_{lo}(s) = 1$ for $s \geq \mathbb{E}[S_y]$ and $g_{hi}(s) = 1$ for $s \leq \mathbb{E}[S_y]$, so $s_y^- \leq \mathbb{E}[S_y]$ and $s_y^+ \geq \mathbb{E}[S_y]$, always. Firstly, however, the most important contributions to the estimate of a particular return level come from each $\mathbb{E}[S_y]$. Secondly, in terms of the effect of

Table 2: CPU time (secs) for simulating from the small, standard and large portfolios. Timings are for the standard method and when using the concentration inequalities that give B_1 and B_2 , and, finally, with B_2 using sampling-importance-resampling (SIR). Timings are reported for obtaining $M = 100$ and $M = 1000$ samples from the loss distribution for all 1000 years. Each complete simulation was repeated 10 times; the table reports the mean and standard deviation of the timings.

Portfolio	M	Std. Method	B_1 direct	B_2 direct	B_2 SIR
small	100	49.2 (0.97)	196 (6.30)	98.2 (3.82)	1.35 (0.056)
standard	100	298 (6.3)	194 (13.2)	108 (9.18)	1.47 (0.239)
large	100	2719 (100)	200 (25.7)	116 (17.2)	1.40 (0.035)
small	1000	511 (25.3)	1845 (235)	965 (142)	2.82 (0.131)
standard	1000	2870 (96.4)	1740 (253)	1070 (152)	2.79 (0.093)
large	1000	26221 (352)	2006 (399)	1119 (214)	2.90 (0.068)

variability, when s_y itself is simulated M times, it is the exceptionally low or high values of u_y and s_y (for each y) that bracket its behaviour; the low values are well represented by the corresponding low values of s_y^- and the high values by the high values of s_y^+ ; the low values of s_y^+ and the high values of s_y^- are rarely important.

As written, each of our concentration inequalities provide an upper bound on $\mathbb{P}(S \geq s)$, which may be used as $g_{hi}(s)$. Applying the same type of bound to $-S$, with associated new values for each c_i , and hence c_* , leads to the bound $g_{lo}(s) \geq \mathbb{P}(-S \geq -s) = \mathbb{P}(S \leq s)$.

By this method, the number of simulations is $\mathcal{O}(Mn_y)$. However, to obtain a single pair of samples, upper and lower bounds on the unobtainable ‘true’ sample, we must solve $g_{lo}(s^-) = u = 1 - g_{hi}(s^+)$. These equations are not even tractable for Bennett’s inequality (4), and require a numerical solution. For B_2 (11) each step of the numerical solver involves an evaluation of Lambert’s W , while for B_1 (10), each step of the solver involves a numerical minimisation over λ .

Table 2 compares the timings for simulation via the standard method and using the inverse cdf method with B_1 and B_2 for 1000 years of floods using our standard portfolio, which has 10^5 risks and approximately 1.8×10^6 subrisks, both using $M = 100$ and $M = 1000$; this is repeated for the small portfolio from which our standard portfolio was derived (see Section 3.2) and for the large portfolio, ten times the size of the standard portfolio. Before simulations can proceed, each method has a set up cost, where the event and portfolio information is read in. For the concentration-based methods, summaries for each year, such as n , $\bar{\sigma}^2$ and K , are also calculated. These pre-simulation *set up* times for the standard method were 0.75 (0.97) for the Small Portfolio, 4.22 (0.31) for the Standard Portfolio and 23.4 (0.63) for the Large Portfolio. The corresponding set-up times for the three portfolios for the concentration methods were: 1.44 (0.052), 6.03 (0.132) and 47.2 (1.52).

Recall that our simulations are for 1000 years of flood events. To give more reliability on estimates of the high return levels it is more typical to simulate from 10000 years of events. The full UK JBA Flood Event Set has an average of 10.6 events per year ³. Also, our

³<https://www.jbarisk.com/products-services/catastrophe-models/event-sets/>

standard portfolio has about 10^5 risks, whereas a large portfolio, for the UK or for the whole of Western Europe, for example, might have 10^6 or more risks. This means that simulations for a large portfolio can take 24 hours or more to complete in practice.

As expected, the CPU time for the standard method scales in proportion to M and, except for the small portfolio, where the relative cost of other overheads is larger, in proportion to the portfolio size. Again, as expected, for all concentration-based methods, there is little dependence on the portfolio size, but direct simulation using B_1 or B_2 has a cost proportional to M . For $M = 1000$, simulating using B_1 takes about 60% of the CPU time that the standard method takes, and simulating B_2 takes about 37% of the CPU time; typically, there is less of an improvement when $M = 100$, and more improvement the larger the portfolio size. Set up costs for B_1 and B_2 are typically twice those for the standard method, but these are dwarfed by the simulation costs.

The table also includes times for simulating from B_2 via an importance sampling-resampling method. For the standard portfolio, this method is a factor of around 200 times faster than the standard method when $M = 100$, with a factor of around 1000 when $M = 1000$. These ratios improve by a further factor of 10 for the larger portfolio. Interestingly the cost of the SIR simulations only doubles when M increases by a factor of 10, presumably due to the vectorisation of the simulation, transformation and weighting operations. We now describe this importance-sampling method.

4.3 Importance sampling-resampling

Importance sampling obtains an approximate, weighted sample, $\{(x_i, w_i)\}_{i=1}^M$, from a distribution with a density of f by simulating a sample, x_1, \dots, x_M , from a distribution with a density of q , called the proposal density, setting $w_i^* = f(x_i)/q(x_i)$ for $i = 1, \dots, n$ and finally setting $w_i = w_i^*/\sum_{j=1}^n w_j^*$. The Monte Carlo representation of the intended distribution is then $\sum_{i=1}^M w_i \delta(x - x_i)$, where δ is Dirac's δ -function. Sampling M times from this weighted approximation to f gives an unweighted sample which can be used to approximate f .

Throughout this exposition we consider simulation from F^+ ; simulation from F^- proceeds analogously. Our proposal distribution is based on Bernstein's inequality:

$$\frac{1}{n} \log \mathbb{P}(S_n \geq nt) \leq -\frac{\bar{\sigma}^2}{c_*^2} \times \frac{\{c_* t / \bar{\sigma}^2\}^2}{2 + 2\{c_* t / \bar{\sigma}^2\} / 3}.$$

From this $P(S_n \geq t') \leq \exp \left[-n \frac{\bar{\sigma}^2}{c_*^2} \frac{v^2}{2+2v/3} \right] =: S_{Ber}(t')$ with

$$v = \frac{c_* t'}{n \bar{\sigma}^2}.$$

Bernstein's inequality is weaker than Bennett's inequality and can be derived directly from it (e.g. Boucheron et al., 2013, Section 2.7). Unlike Bennett's inequality, however, it is straightforward to sample from the Bernstein approximation, solving $S_{Ber}(t') = u$ to obtain

$$t' = \left[\left\{ \frac{1}{3} c_* \log u \right\}^2 - 2n \bar{\sigma}^2 \log u \right]^{1/2} - \frac{1}{3} c_* \log u.$$

Differentiation of $S_{Ber}(t')$ gives the proposal density:

$$q(t') = \frac{2}{c_*} \frac{v(2+v/3)}{(2+2v/3)^2} S_{Ber}(t').$$

We consider $S_{BS} := \exp\{nB - \lambda t'\}$ with B as defined in (8), for which

$$f_{BS}(t') = \left[\left\{ n \frac{dB}{d\lambda} - t' \right\} \frac{d\lambda}{dt'} - \lambda \right] S_{BS}(t').$$

It is straightforward to show that $\frac{d}{d\lambda} \lambda^j f_j(\lambda c_*) = \lambda^{j-1} f_{j-1}(\lambda c_*)$, from which:

$$\frac{dB}{d\lambda} = \lambda(\overline{\sigma^2} - K) + K\lambda f_1(\lambda c_*) - K_1 c_*^2 \lambda^3 f_3(\lambda c_*).$$

We have not been able to obtain $d\lambda/dt'$ corresponding to the numerical solution for λ in (10); however for (11) Appendix C shows that

$$\frac{d\lambda}{dt'} = \frac{1}{n(\overline{\sigma^2} - K)} \times \frac{1}{1 + W},$$

where

$$W = \mathcal{W} \left(\frac{K}{\overline{\sigma^2} - K} \exp \left[\frac{K + t' c_*/n}{\overline{\sigma^2} - K} \right] \right). \quad (23)$$

The importance-sampling-resampling method, requires only a single evaluation of \mathcal{W} per sample and leads to the impressive speed up illustrated in Table 2. Figures 1 and 2 show that the bound B_2 from (11) is close to B_1 from (10). We, therefore, recommend using importance-sampling-resampling with bound B_2 .

Strictly speaking, the unweighted sample obtained by sampling-importance-resampling is not a sample from f but its distribution tends to that of a sample from f as $M \uparrow \infty$. To improve the accuracy of the sample we use residual resampling (e.g. Doucet and Johansen, 2011). Figures 6 and 7 in Appendix D demonstrate empirically that in our examples the samples are visually indistinguishable from a sample from f .

4.4 Numerical comparison

We now compare results from the standard method with those from our importance sampling-resampling method using bound B_2 . Estimating a 95% prediction interval using only $M = 100$ realisations leads to considerable Monte Carlo variability, so to mitigate for this source of variability, we use $M = 1000$ throughout this comparison.

The left panel of Figure 4 shows the estimated k year return levels for $k=2, 5, 10, 20, 50, 100, 200, 500$. The first plot shows that the estimates obtained from B_2 closely track the estimates from the standard method. The second plot shows that the intervals when using B_2 are wider than those obtained by the standard method, but that they get narrower as the return level increases. From the 10-year return level upwards, both the upper and lower point estimates are within 5% of the point estimate from the standard method, reducing to 2% for the 100-year and higher return levels. Similarly, from the 10-year return level, the

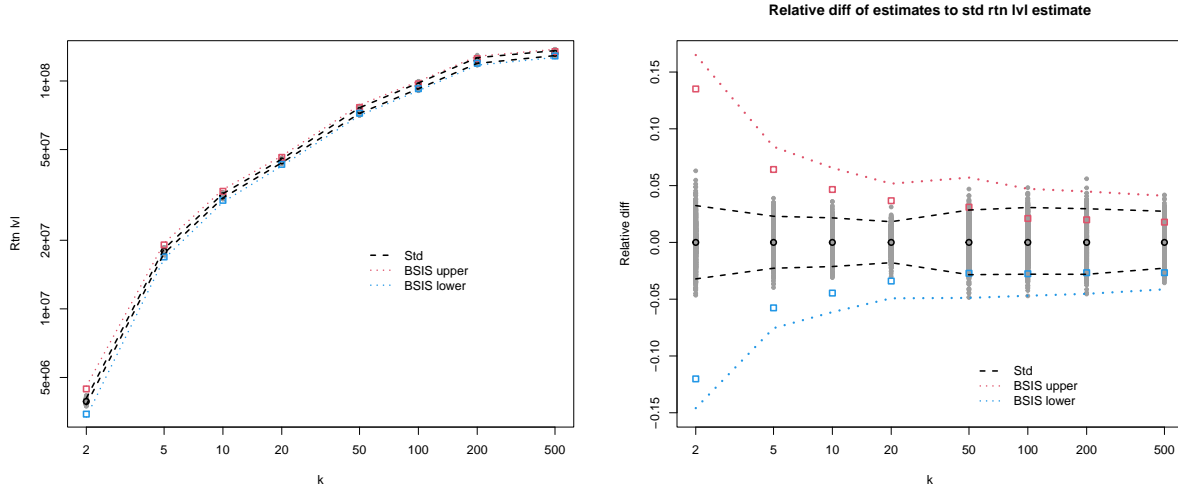


Figure 4: Return level point estimates and 95% predictive bounds via the standard method (in black) and via sampling importance resampling using bound B_2 for F^+ and F^- . The point estimate and upper end of the prediction interval when using F^+ appear in red; when using B_2 for F^- , the corresponding point estimate and lower predictive bound appear in blue. The first plot shows the raw return level predictions; the second plot shows the values, v , relative to the point estimate, s , from the standard method: $(v - s)/s$. On the second plot, the 1000 realisations from the standard method appear in grey.

Table 3: Relative width of the 95% prediction interval for each return level from the concentration approach compared with the standard method.

Return level	2	5	10	20	50	100	200	500
Relative width	5.099	3.448	2.928	2.713	1.880	1.624	1.577	1.546

estimates of the prediction bounds are within around 5% of the bounds obtained from the standard method, reducing to a few percent from the 100-year level. Errors in estimating the two-year return level, especially, are more substantial.

Table 3 shows for each return level the relative width of the 95% prediction interval obtained via our conservative methodology to that of the interval obtained using the standard method. This ratio is large for the two-year return level and decreases with increasing return level. For the 5-year return level it is less than a factor of 3.5 and for the 50-year return level and above it is less than a factor of 2.

Figure 8 in Appendix E repeats the second plot in Figure 4 but with a different random seed for the standard portfolio, and then for the large portfolio. Both show the same overall pattern that is seen in Figure 8, but we highlight two changes with the larger portfolio. Firstly, the relative differences are smaller, as would be expected since yearly expected losses are proportional to n , the portfolio size, whereas standard deviations are proportional to \sqrt{n} . Furthermore, the discrepancies between the predicted CIs using B_2 and those using the standard method are slightly smaller.

Figure 2 shows a substantial deviation between the loss from B_2 and B_{lb} for the year (A) with lower quartile expected loss. The upper tails of years with the lower expected losses will impact the lower return levels and we conjecture that for these years, a tighter concentration bound, as discussed in Section 5.1 and Appendix A, might lead to narrower intervals for the lower return levels.

5 Discussion

Repeated simulations of individual losses for each subrisk over an entire portfolio for each of 1000 or 10000 years worth of flood events is computationally very costly. We have described a new methodology, based upon a new concentration inequality, that gives upper and lower bounds on the simulated yearly losses and reduces the computation by orders of magnitude. We first discuss the new concentration inequalities, then the new simulation methodology.

5.1 The concentration inequalities

Our new inequalities, (10) to (12), are extensions of Bennett’s inequality (4). As with Bennett’s inequality, the support of individual variables to be summed has a finite upper bound, and the individual variances are taken into account. In contrast to Bennett’s inequality which employs a single upper bound on the supports of all the variables, our bounds account for the individual supports. Our tightest bound (10) requires numerical optimisation, but both (11) and (12) are tractable via Lambert’s W-function.

If it is known that all $c_i \geq c_0 > 0$ then a tighter bound may be obtained from an analog of Lemma 1 by interpolating h_J between λc_0 and λc_* rather than between 0 and λc_* . Even removing the K_1 term, this does not lead to a tractable minimisation problem, but the bound may still be efficiently minimised numerically with respect to λ . In scenarios of interest to us, $c_0 \ll c_*$ and the gains are negligible.

A stronger tightening of (8) is possible at the expense of evaluating more summary statistics of the form $K_j = (1/n) \sum_{i=1}^n \sigma_i^2 (c_i/c_*) (1 - c_i^j/c_*^j)$. A brief derivation of this sequence of bounds is given in Appendix A. The new bounds can only be substantially tighter if the K_j , $j \geq 2$, are substantially larger than K_1 . Across toy scenarios (i) to (iv) from Section 3.1, K_2/K_1 varied between 1.23 and 1.36, and K_3/K_2 varied between 1.06 and 1.11, showing quickly diminishing returns, which is unsurprising since our entire motivation was that for many subrisks, $c_i \ll c_*$. In other scenarios, the bound on further improvement, obtained through (15), could inform a decision on gathering further summaries.

Alternative tightenings of Bennett’s inequality are possible in cases where σ_i/c_i has a non-trivial lower or upper bound. For the former, see Equation 2c of Bennett (1962); for the latter, note that terms in the sum in (16) can be rewritten as $\{\exp(\lambda c_i) - 1\} \sigma_i^2/c_i^2$. An especially low upper bound on σ_i/c_i could reward taking this outside the sum and setting $h(u) = \exp(u) - \sum_{j=2}^{\infty} u^j/j!$. Over a portfolio, the probability of flooding can, and usually does, take values over the whole range between 0 and 1, so neither of these approaches is helpful in our application.

Similar ideas to those used in the proof of Lemma 1 can create successive improvements on a generalisation of Theorem 1 of Hoeffding (1963) (see Barlow, 2021). However, at least in scenarios of interest to us, these did not improve upon Lemma 1, and so we do not include them in any more detail here.

Theorem 1.3 of Bentkus (2004) provides a Hoeffding-like bound that only requires an upper bound on the support, but in cases of interest to us is looser than the bound of Hoeffding. Light (2021) uses moment information from the individual X_i to improve upon both Hoeffding’s inequality and Bennett’s inequality. The Hoeffding improvement is potentially useful when the X_i are identically distributed or when there are a few fixed t values of interest. When the variables are not identically distributed, evaluating $\mathbb{P}(S_n > nt)$ requires a fresh $\mathcal{O}(n)$ calculation for each new t . When simulating via the inverse-cdf method we must find the minimum t such that $\mathbb{P}(S_n \geq t) \leq \epsilon$, numerical solution of the equation would require many $\mathcal{O}(n)$ calculations, which we wish to avoid.

5.2 Methodology and comparison

When using (10) for simulation via the inverse-cdf method, each of the n_{step} steps of a numerical solver of the two equations $F^+(s^+) = u = F^-(s^-)$ requires a numerical minimisation. This is then repeated for each of the $n_y \in \{1000, 10000\}$ years and then the whole set of calculations is replicated $M \in \{100, 1000\}$ times. Even though the individual minimisations are $\mathcal{O}(1)$, not $\mathcal{O}(n)$ (where n is the size of the portfolio), Table 2 shows that this is computationally expensive. Indeed, $n_{step} \times n_y \times M$ evaluations of Lambert’s W as used in (11) is also only a small factor cheaper than the $\mathcal{O}(n)$ calculations used in the standard method. The sampling-importance-resampling methodology employs a tractable proposal distribution based on a well-known loosening of Bennett’s inequality and reduces the number of minimisations or evaluations of Lambert’s W to $n_y \times M$; Table 2 shows the very substantial consequent gain in computational efficiency.

These simulations lead to conservative prediction intervals of the k -year return levels for various k . In our simulations, except for the two-year return level, the new intervals are between a factor of 1.5 and 3.5 times as wide as the intervals obtained via the standard method, with the ratio decreasing as the return level increases.

Both the standard method and our method estimate return levels based upon statistical models which are imperfect representations of reality. The nature and number of flood events in a given year are simulated from a particular extreme-value model fitted to partially-observed data. Moreover, the distribution of the fraction of the insured value that will be claimed if a subrisk is flooded will vary between subrisks and, in reality, these distributions may not be entirely independent. Finally, the simulation method takes no account of parameter uncertainty. In the event of model uncertainty and incomplete observations Copas and Eguchi (2005) suggest multiplying prediction intervals by approximately $\sqrt{2}$; the same might be expected to hold for our intervals even before accounting for parameter uncertainty. Our method, by design, produces wider intervals than those obtained by assuming that the model is true and that there is no parameter uncertainty and, on our portfolio, the increase in width varies between a factor of 1.5 and 2 for return levels above and including the 50-year level (see Table 3). Whilst the mechanism by which our

method produces wider prediction intervals is not intended to be a representation of model and parameter uncertainty, it does produce intervals of a relative size that fits with the rough increase in width one might expect if these uncertainties were taken into account. We, therefore suggest that it is, at the very least, not unreasonable to work with these intervals.

5.3 Alternative approaches

At first glance, two natural potential alternatives to our procedure suggest themselves. We describe both possibilities and explain why neither is suitable for our purposes.

If upper and lower concentration inequalities were available for the order statistics of the yearly losses for the collection of 1000 or 10000 years outputted by the flood-event model, rather than for the individual losses themselves, then bounds on the quantiles for the relevant losses could be obtained directly from the inequalities without any simulation. For example, concentration inequalities on the 100th highest loss of a total of 1000 years outputted from the flood-event model would provide upper and lower bounds on the point estimate and quantiles of the 10-year return level. The only work of which we are aware of in this area is Boucheron and Thomas (2012), which derives concentration inequalities for independent and identically distributed random variables whose cumulative distribution function has a known functional form and, for most of the inequalities, the random variables can be represented by a density with a non-increasing hazard. None of these conditions holds in our case, and any generalisation to include our scenario would require substantial work if it were even possible.

In some scenarios (e.g. Scott and Metzler, 2015, and references therein) it is possible to apply importance sampling to the generation of “events”, so that fewer non-extreme events and more extreme events are generated. Each generated event is then given a weight: the ratio of the density of the outcome under the generative model that is assumed to be a truth and under the model that favours more extreme years. In our situation the model that generates a single flood event over the region of space covered by an entire portfolio is very complex, involving simulation of a particularly extreme location to be conditioned on and then back-transformation via a different empirical cumulative distribution function at each of thousands of river gauge locations spanning the portfolio region (Lamb et al., 2010; Keef et al., 2013; Towe et al., 2019). This output is then spatially interpolated to the locations of all the risks in the portfolio; for each risk, the interpolated level is combined with information about the risk (such as elevation) to give a probability of flooding and a beta distribution for the fraction of the insured value lost if a flood occurs; simulating from this distribution for each subrisk at the risk and summing gives the loss at that risk, and summing over all risks gives the total loss for the event. The number of events in a year usually simulated from a Poisson distribution; summing over all events in a year gives the loss for that year. The true density/mass function for the loss distributions for a given year is, therefore, not tractable. Even if it were tractable, it would be far from straightforward to create a suitable proposal distribution for the joint distribution across all risks of the flood probabilities and beta parameters for each risk. Moreover, importance sampling is typically used for a particularly high quantile, such as the 0.999th. The resulting proposed events and years worth of events are then, typically, not suitable for estimating much less

extreme quantiles. We are interested in return levels from the two-year (0.5 quantile) and up, so a careful balance between the gain in efficiency for high quantiles and the loss of efficiency for low quantiles would need to be maintained.

Acknowledgements

Work by the first author was supported by EPSRC grant numbers EP/L015692/1 and EP/S000747/1, and JBA Risk Management.

References

- Barlow, A. M. (2021). *Flood Events: Extreme Value Problems and Efficient Estimation of Loss*. PhD thesis, Lancaster University, UK.
- Bennett, G. (1962). Probability inequalities for the sum of independent random variables. *Journal of the American Statistical Association*, 57(297):33–45.
- Bentkus, V. (2004). On Hoeffding’s inequalities. *The Annals of Probability*, 32(2):1650 – 1673.
- Bentkus, V. and Juškevičius, T. (2008). Bounds for tail probabilities of martingales using skewness and kurtosis. *Lithuanian Mathematical Journal*, 48(1):30–37.
- Boucheron, S., Lugosi, G., and Massart, P. (2013). *Concentration Inequalities: A Nonasymptotic Theory of Independence*. Oxford University Press, Oxford.
- Boucheron, S. and Thomas, M. (2012). Concentration inequalities for order statistics. *Electronic Communications in Probability*, 17(none):1 – 12.
- Copas, J. and Eguchi, S. (2005). Local Model Uncertainty and Incomplete-Data Bias (With Discussion). *Journal of the Royal Statistical Society Series B: Statistical Methodology*, 67(4):459–513.
- Corless, R. M., Gonnet, G., Hare, D., Jeffrey, D., and Knuth, D. (1996). On the Lambert W function. *Advances in Computational Mathematics*, 5:329–359.
- Doucet, A. and Johansen, A. (2011). A tutorial on particle filtering and smoothing: fifteen years later. In Crisan, D. and Rozovsky, B., editors, *The Oxford Handbook of Nonlinear Filtering*. Oxford University Press.
- Hoeffding, W. (1963). Probability inequalities for sums of bounded random variables. *Journal of the American Statistical Association*, 58(301):13–30.
- Keef, C., Tawn, J. A., and Lamb, R. (2013). Estimating the probability of widespread flood events. *Environmetrics*, 24(1):13–21.
- Lamb, R., Keef, C., Tawn, J., Laeger, S., Meadowcroft, I., Surendran, S., Dunning, P., and Batstone, C. (2010). A new method to assess the risk of local and widespread flooding on rivers and coasts. *Journal of Flood Risk Management*, 3(4):323–336.

- Light, B. (2021). Concentration inequalities using higher moments information. arXiv.
- Pinelis, I. (2014). On the Bennett–Hoeffding inequality. *Annales de l’Institut Henri Poincaré, Probabilités et Statistiques*, 50(1):15 – 27.
- Pinelis, I. S. and Utev, S. A. (1990). Exact exponential bounds for sums of independent random variables. *Theory of Probability & Its Applications*, 34(2):340–346.
- Scott, A. and Metzler, A. (2015). A general importance sampling algorithm for estimating portfolio loss probabilities in linear factor models. *Insurance: Mathematics and Economics*, 64:279–293.
- Swain, R. and Swallow, D. (2015). The prudential regulation of insurers under solvency ii. *European Economics: Macroeconomics and Monetary Economics eJournal*.
- Taylor, P. and Carter, J. (2020). Oasis financial module. Technical report, Oasis Loss Modelling Framework Ltd. Version 3.
- Towe, R. P., Tawn, J. A., Lamb, R., and Sherlock, C. G. (2019). Model-based inference of conditional extreme value distributions with hydrological applications. *Environmetrics*, 30(8):e2575. e2575 env.2575.
- Zheng, S. (2018). An improved Bennett’s inequality. *Communications in Statistics - Theory and Methods*, 47(17):4152–4159.

A Further tightening of the bound (8)

As alluded to in the discussion, (8) may be tightened still further provided additional summaries are created.

When simplifying (17), for a fixed $J \geq 1$,

$$\begin{aligned}
u^2 \sum_{j=0}^{\infty} \frac{u^j}{(j+4)!} &= u^2 \sum_{j=0}^{J-1} \frac{u^j}{(j+4)!} + u^{2+J} \sum_{j=0}^{\infty} \frac{u^j}{(j+4+J)!} \\
&\leq u^2 \sum_{j=0}^{J-1} \frac{u^j}{(j+4)!} + u^{2+J} \sum_{j=0}^{\infty} \frac{u_*^j}{(j+4+J)!} = u^2 \sum_{j=0}^{J-1} \frac{u^j}{(j+4)!} + u^{2+J} f_{4+J}(u_*).
\end{aligned} \tag{24}$$

Similarly

$$uu_* \sum_{j=0}^{\infty} \frac{u_*^j}{(j+4)!} = uu_* \sum_{j=0}^{J-1} \frac{u_*^j}{(j+4)!} + uu_*^{1+J} f_{4+J}(u_*).$$

For $J \geq 1$, this leads to the tighter limit of

$$f_2(u) \leq f_2(0) + \frac{u}{u_*} \{f_2(u_*) - f_2(0)\} - \frac{u}{u_*} \sum_{j=0}^{J-1} \frac{u_*^{j+2}}{(j+4)!} \left\{1 - \frac{u^{j+1}}{u_*^{j+1}}\right\} - \frac{u}{u_*} \left\{1 - \frac{u^{J+1}}{u_*^{J+1}}\right\} u_*^{J+2} f_{J+4}(u_*).$$

The bound (8) then becomes

$$\frac{1}{2}\lambda^2\overline{\sigma^2} + \lambda^2 K \left\{ f_2(\lambda c_*) - \frac{1}{2} \right\} - \sum_{j=0}^{J-1} \frac{K_{j+1}}{(j+4)!} \lambda^{j+4} c_*^{j+2} - K_{J+1} \lambda^{J+4} c_*^{J+2} f_{J+4}(\lambda c_*),$$

where $K_j = \sum_{i=1}^n \sigma_i^2 \frac{c_i}{c_*} \left(1 - \frac{c_i}{c_*}\right)^j$ generalises the definition of K_1 .

B Additional Figures

Figure 5 is the converse of Figure 2, estimating $\frac{1}{n}\mathbb{P}(S_n - \mathbb{E}[S_n] \leq -nt)$ rather than $\frac{1}{n}\mathbb{P}(S_n - \mathbb{E}[S_n] \geq nt)$. The results for the lower tail are so different to those for the upper tail for the years with lower expected total cost because the distributions of the total cost are skewed. For example, the skewness for four years in order, estimated from 20000 simulations, are approximately +1.20 and +0.47, +0.18 and 0.08 respectively.

C Derivation of $d\lambda/dt$

From (14),

$$\lambda = \frac{1}{c_*} \left[r(t) - \mathcal{W} \left(\frac{nK}{c_*} r'(t) \exp[r(t)] \right) \right] \quad \text{where} \quad r(t) = \frac{K + tc_*/n}{\overline{\sigma^2} - K}.$$

Since $r''(t) = 0$,

$$\frac{d\lambda}{dt} = \frac{1}{c_*} \left[r'(t) - \frac{nK}{c_*} \{r'(t)\}^2 \exp[r(t)] \mathcal{W}' \left(\frac{nK}{c_*} r'(t) \exp[r(t)] \right) \right] = \frac{r'(t)}{c_*} [1 - x \mathcal{W}'(x)],$$

where $x = \frac{nK}{c_*} r'(t) \exp[r(t)]$.

But, by definition, $x = W \exp(W)$, where $W = \mathcal{W}(x)$, so $dx/dW = (W + 1) \exp(W) = (W + 1)x/W$, so $x \mathcal{W}'(x) = W/(1 + W)$. Thus

$$\frac{d\lambda}{dt} = \frac{r'(t)}{c_*} \frac{1}{1 + W} = \frac{1}{n(\overline{\sigma^2} - K)} \times \frac{1}{1 + W},$$

where W is as defined in (23).

D Comparison of importance sampling-resampling with direct simulation

For each of the four representative years from Section 3.2, Figure 6 compares the true bound, B_2 , against estimates of it via Monte Carlo simulation using the direct method

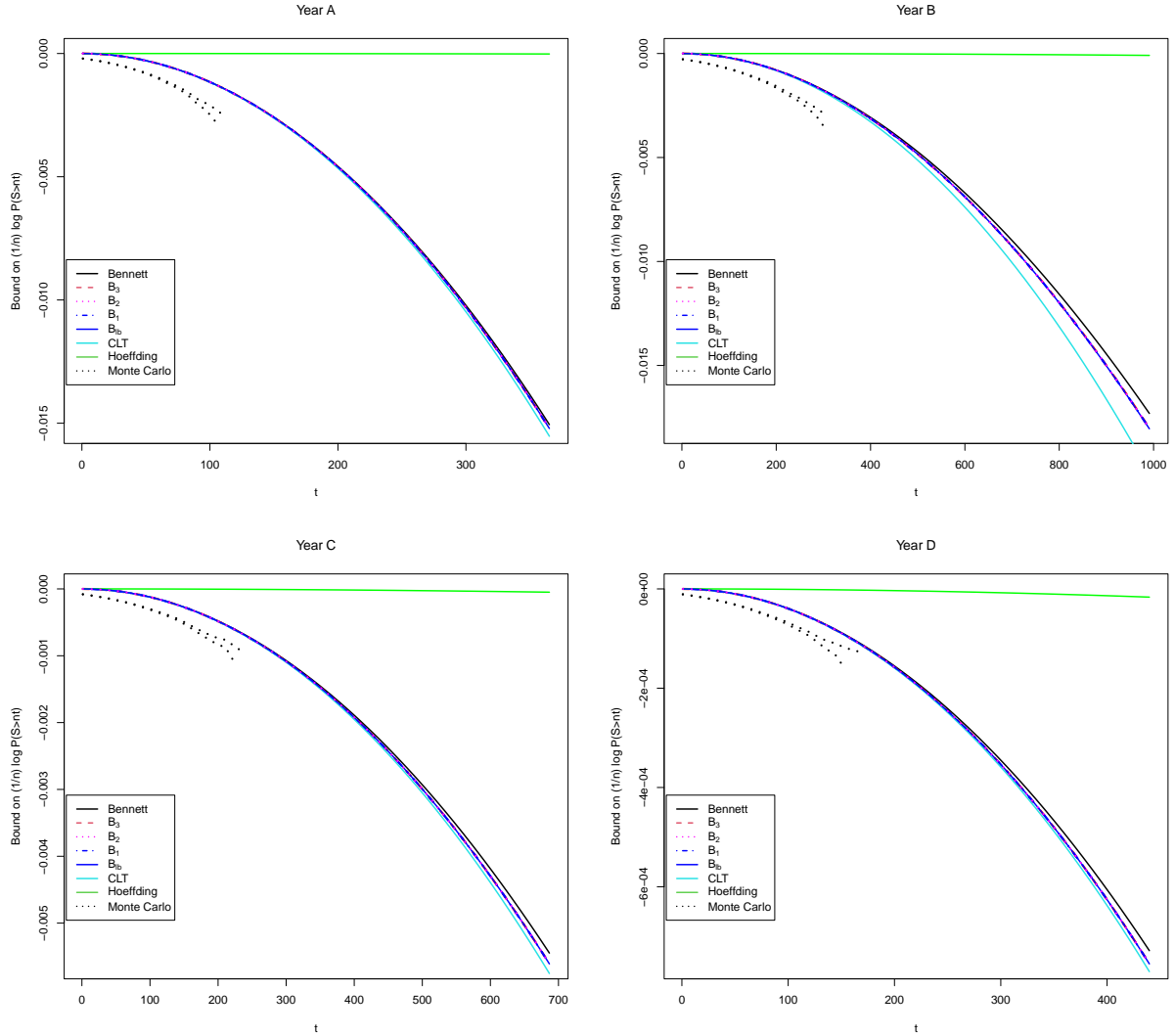


Figure 5: Comparison of bounds on $\frac{1}{n} \log \mathbb{P}(S_n - \mathbb{E}[S_n] \leq -nt)$ plotted against t : Bennett (black solid); Equation (10), denoted B_1 , in blue dot-dash and Equation (12), denoted B_3 , in red dashed. Other solid lines are: the large- n approximation from the central limit theorem (cyan) and the Hoeffding bound (green). The dotted magenta lines show 90% CIs based on 20000 Monte Carlo simulations from the true distribution. The four panels correspond, respectively, to Years A, B, C and D.

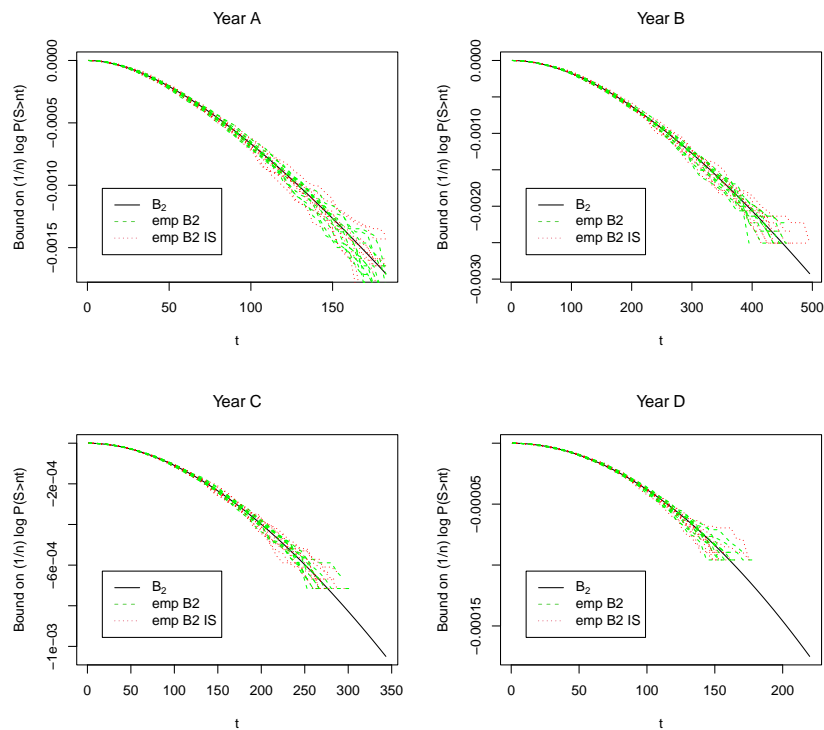


Figure 6: Comparison for each of the four representative years of the bound B_2 and empirical estimates of the bound by ten replicates of 1000 simulations from the loss for that year via the B_2 bound, both via direct sampling (green) and via sampling-importance-resampling (red). The lines cut off when the empirical estimate of the probability is $1/1000$.

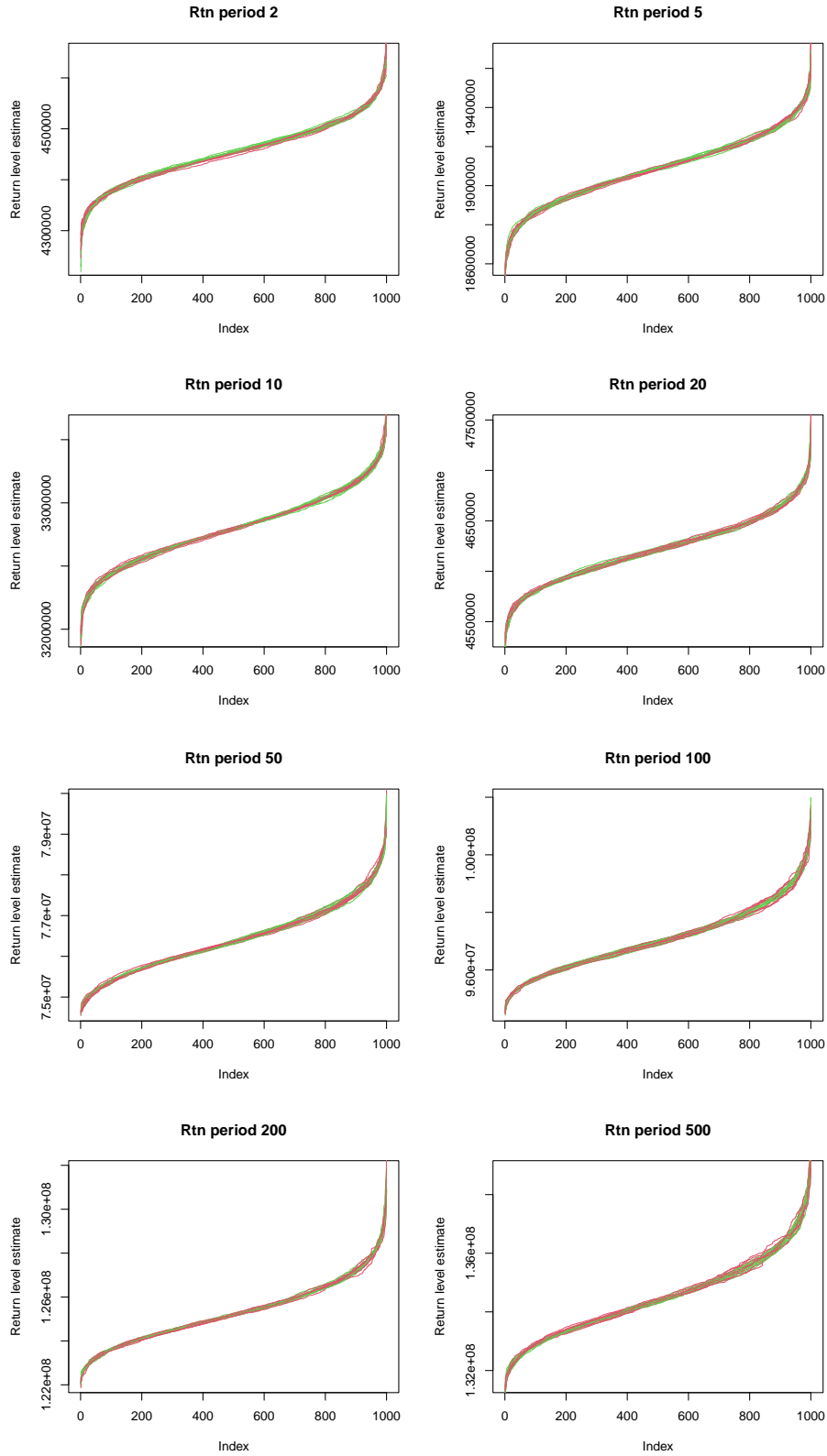


Figure 7: Comparison of simulations of the upper bound on the k -year return level using B_2 by direct sampling (green) and importance sampling-resampling (red). Each plot corresponds to a particular return period and shows ten replicate lines for each bound, each line is derived from 1000 simulations, ordered by the simulated value.

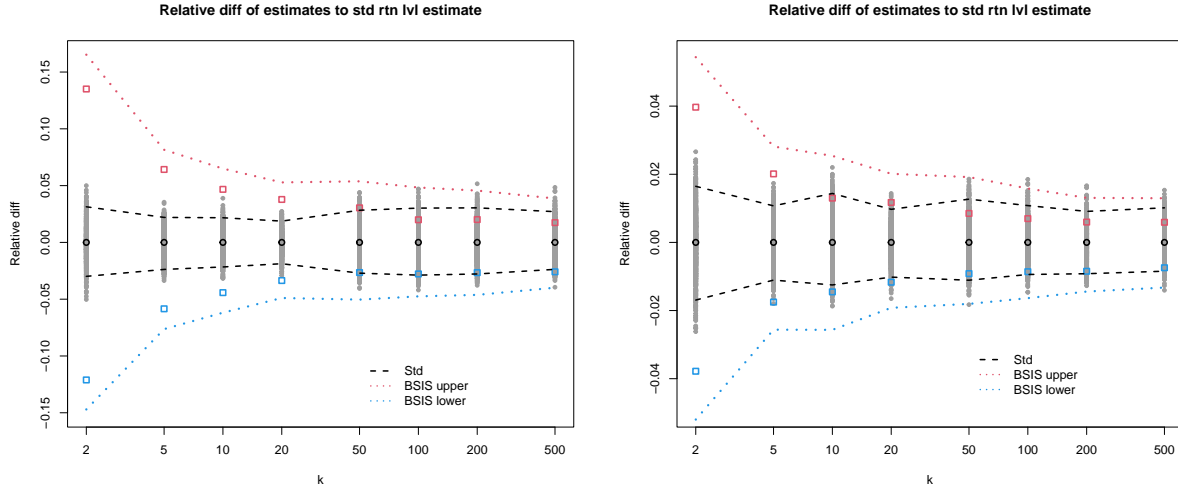


Figure 8: Relative return level point estimates and 95% predictive bounds via the standard method (in black) and via sampling importance resampling using bound B_2 for F^+ and F^- . The point estimate and upper end of the prediction interval when using F^+ appear in red; when using B_2 for F^- , the corresponding point estimate and lower predictive bound appear in blue. Values are relative to the point estimate from the standard method, s ; *i.e.*, $v \rightarrow (v - s)/s$. The first is for the standard portfolio using a different random seed to that which generated the results in Figure 7. The second plot is for the larger portfolio. In both plots, the 1000 realisations from the standard method appear in grey.

and using sampling-importance-resampling. For each year, each simulation method leads to similar variability about the true probability under B_2 .

Figure 7 compares the return-level distributions obtained from simulations from all 1000 years using direct simulation and then using sampling-importance-resampling, and suggests that any discrepancies between the distributions are small and, except for the two-year return levels, (at most) of a similar magnitude to the Monte Carlo variability between replicates.

E Further return-level estimates

Figure 8 repeats the second plot in Figure 4 but with a different random seed, and shows the same overall pattern. It then repeats this plot again but for the large portfolio. The overall pattern is the same as for the standard portfolio, but we highlight two changes. Firstly, the relative differences are smaller, as would be expected since yearly expected losses are proportional to n , the portfolio size, whereas standard deviations are proportional to \sqrt{n} . Furthermore, the discrepancies between the predicted CIs using B_2 and those using the standard method are smaller.